

## Zoned Fishnet Lens Antenna with Reference Phase for Side Lobe Reduction

V. Pacheco-Peña, M. Navarro-Cía, B. Orazbayev, I.V. Minin, O.V. Minin and M. Beruete

**Abstract**— Reduction of first side lobe level and nulls in artificial fishnet metalenses is accomplished here by applying the reference phase concept along with the zoning technique. Higher focusing efficiency is achieved for a specific reference phase when comparing numerically and experimentally four different designs. For such best design, an improvement of the first side lobe level ( $\sim 2.4$  dB), first null ( $\sim 13$  dB) and gain ( $\sim 1.77$  dB) is achieved experimentally compared to the design without reference phase.

**Index Terms**— Zoned lenses, Fresnel zoning, lens antennas, millimeter-waves, fishnet metamaterial.

### I. INTRODUCTION

REDUCING the first side lobe level (SLL) and cross-polarization of lens antennas at millimeter-waves without perturbing the rest of radiation parameters is usually challenging. Since the origin of the side lobes and cross-polarization is frequently due to the large free-space impedance mismatch of commonly used materials such as high-resistivity silicon [1], one possible solution is to use materials with lower dielectric permittivity. However with such materials a thicker lens profile is required. Alternatively, graded index lenses could be used [2]. Nevertheless, this solution remains elusive with dielectrics at millimeter-waves because of fabrication challenges and has only been achieved so far with metamaterial lenses, i.e., metalenses [3], [4].

The fishnet metalens with double in-plane periodicity minimizes the impedance mismatch with free-space and intrinsically filters the cross-polarization component [5], [6]. Unfortunately, the fishnet metalens may be bulky and heavy for some applications. A lightweight fishnet metalens can be designed by exploiting the concept of Fresnel zoning [7]–[9],

Manuscript received March 31, 2015. This work was supported in part by the Spanish Government under Grant Consolider “Engineering Metamaterials” CSD2008-00066, TEC2011-28664-C02-01. V.P.-P. is sponsored by Spanish Ministerio de Educación, Cultura y Deporte under grant FPU AP-2012-3796. M. N.-C. is supported by the Imperial College Junior Research Fellowship. B.O. is sponsored by Spanish Ministerio de Economía y Competitividad under grant no. FPI BES-2012-054909. M. B. is sponsored by the Spanish Government via RYC-2011-08221.

V. Pacheco-Peña, V. Orazbayev and M. Beruete are with Antennas Group-TERALAB, Universidad Pública de Navarra, Pamplona 31006, Spain (e-mail: victor.pacheco@unavarra.es, b.orazbayev@unavarra.es, miguel.beruete@unavarra.es).

M. Navarro-Cía is with the Optical and Semiconductor Devices Group, Department of Electrical and Electronic Engineering; Centre for Plasmonics and Metamaterials; and Centre for Terahertz Science and Engineering, Imperial College London, London SW7 2AZ, UK. He is also with the Department of Electronic & Electrical Engineering, University College London, London WC1E 7JE, UK (e-mail: m.navarro@imperial.ac.uk).

I.V. Minin and O.V. Minin are with the Siberian State Institute of Metrology, Dimitrova 4, Novosibirsk 630004, Russia (e-mail: prof.minin@gmail.com).

whereby material causing redundant  $2\pi$  phase variation is removed from the lens. This time-honored concept [10], [11] reduces the profile and the weight of a lens at the expense of single frequency operation. Since the fishnet metamaterial is intrinsically narrowband, the zoning does not have any impact in the bandwidth of operation. The zoned design, however, still faces the problem of shadowing effects at the zone boundaries, which deteriorates the gain of the lens antenna system. This can be minimized by designing the fishnet metalens to operate near the zero refractive index regime [7], [8].

Given the success in translating the zoning technique to the fishnet metalens, it can be argued that advanced designs can benefit at full from other concepts developed for Fresnel zone plate antennas [10]. For instance, the concept of reference phase [12], whereby an extra phase advance between 0 and  $\pi$  is added to the central ring of the lens antenna (where 0 is the value that has been commonly used), could lower the first SLL of the fishnet metalens while the rest of radiation characteristics remains unchanged.

We evaluate here the performance of the recently proposed zoned fishnet metalens antennas when different reference phases are considered in the design. Four different values of reference phase (0,  $0.7\pi$ ,  $1.4\pi$  and  $2\pi$ ) determined by the unit cell longitudinal period (fixed by technological constraints) are evaluated. The numerical results show that  $0.7\pi$  is the best case among them for focusing efficiency. We then compare numerically and experimentally the radiation characteristics of two metalens antennas, one with a reference phase of  $0.7\pi$  and another with a value of 0 (i.e., no reference phase). We report a drop in the first SLL of  $\sim 4$  and  $\sim 2.5$  dB according to the simulation and experiment, respectively, without deteriorating the rest of radiation characteristics.

### II. LENS DESIGN

#### A. Reference phase and zoning technique

In a zoned design assuming zero reference phase, the profile of the lens is reduced each time a thickness limit [ $t = \lambda_0 / (1 - n_{lens})$ ], where  $\lambda_0$  is the free-space wavelength and  $n_{lens}$  the refractive index of the lens; notice that this equation is valid for  $n_{lens} < 1$ ] is reached [7]–[9]. When a reference phase is taken into account, the lens profile is stepped up to a thickness limit:

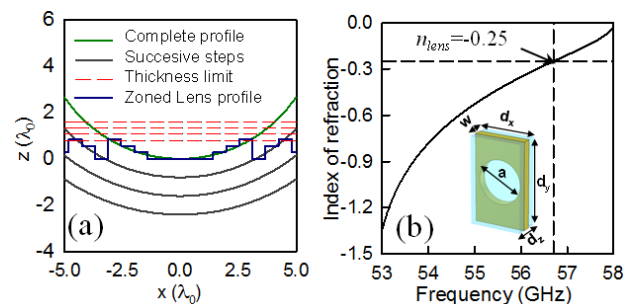


Fig. 1. (a) Example of the zoned lens profile when no reference phase is used (blue line) along with the complete profile (green line), successive steps (gray lines) and thickness limit for a reference phase of 0,  $0.7\pi$ ,  $1.4\pi$  and  $2\pi$  (red-dashed lines) from bottom to top, respectively. (b) Effective refractive index of the fishnet along with the unit cell (inset).

$$t_{total} = t + \Delta t = \frac{\lambda_0}{1 - n_{lens}} + q \frac{\lambda_0}{1 - n_{lens}} \quad (1)$$

where  $\Delta t$  is the extra thickness introduced due to the reference phase and  $q$  is a factor between 0 and 1 which corresponds to an additional phase advance from 0 to  $2\pi$ . The zoned profile of the lens can be obtained by simply using the general equation of a conical section [11], [13], as we did in our previous works [7]–[9] along with the condition of maximum thickness  $t_{total}$  (see Fig. 1(a) for a sketch of the methodology):

$$z = \text{mod} \left[ \frac{FL(1 - n_{lens}) - \sqrt{FL^2(1 - n_{lens})^2 - x^2(1 - n_{lens})^2}}{(1 - n_{lens})^2}, t_{total} = t(q + 1) \right] \quad (2)$$

where  $z$  is the thickness of the lens at the position  $x$ ,  $\text{mod}$  is the modulus operation, and  $FL$  is the focal length.

### B. Zoned fishnet metalenses with reference phase

The fishnet metamaterial used in this manuscript consists of periodically stacked hole arrays with a unit cell with the following parameters: hole diameter  $a = 2.5$  mm, metal thickness (aluminum)  $w = 0.5$  mm and  $d_x = 3$  mm,  $d_y = 5$  mm and  $d_z = 1.5$  mm as the periodicities along  $x$ ,  $y$  and  $z$  axis, respectively, see Fig. 1(b). Air has been chosen as interspacing layer along  $z$  in order to design a free-standing fishnet without unnecessary dielectric losses. Note that  $d_z$  comprises the metal thickness ( $w$ ) and the air layer of 1 mm. The effective refractive index ( $n_{lens} = n_{fishnet}$ ) of an infinite stack of such evenly-spaced two-dimensional holey layers shows negative values from  $\sim 53$  GHz to  $\sim 58$  GHz for vertically-polarized waves (polarized along  $y$ -axis), [7]–[9], [14]. Propagation is forbidden for the orthogonal polarization in that frequency range. With the aim to reduce  $t_{total}$  and thus, minimize the shadowing,  $f = 56.7$  GHz ( $\lambda_0 = 5.29$  mm) is chosen where  $n_{lens} = n_{fishnet} = -0.25$ . A smaller  $t_{total}$  could theoretically be achieved with a smaller (close to zero) refractive index, but then the design would operate close to the band edge, where losses increase.

All the cylindrical fishnet metalenses (with translation symmetry along  $y$ ) are designed with a  $FL = 4.5\lambda_0$  and a focal length to lateral size ratio of  $F/D_{xz} = 0.214$  and  $F/D_{yz} = 0.207$  in the  $xz$ - and  $yz$ - planes, respectively, where  $D_{xz}$  and  $D_{yz}$  are the lateral size of the lens in the  $xz$ - and  $yz$  planes, respectively, to follow the standard -12 dB value of edge taper criterion [15]. For the design frequency ( $f = 56.7$  GHz,  $n_{lens} = -0.25$ ) the thickness limit is  $t = 0.8\lambda_0$ . Since  $\Delta t$  must be multiple of  $d_z = 1.5$  mm  $\sim 0.35t$  to be realizable with our fishnet, the four possible values of  $q$  are evaluated here:  $q = 0, 0.35, 0.7$  and  $1$ , which correspond to a reference phase of  $0, 0.7\pi, 1.4\pi$  and  $2\pi$ , respectively; i.e., an extra thickness ( $\Delta t$ ) of  $0, 0.28\lambda_0, 0.56\lambda_0$

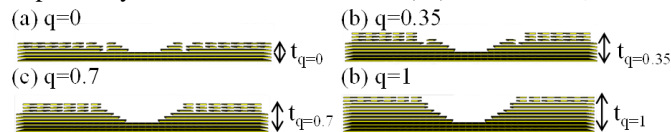


Fig. 2. Top view of the zoned fishnet metalenses under study using different reference phase factors: (a)  $q=0$ , (b)  $q=0.35$ , (c)  $q=0.7$  and (d)  $q=1$  with a total thickness of  $t_{q=0} = 1.51\lambda_0$ ,  $t_{q=0.35} = 2.36\lambda_0$ ,  $t_{q=0.7} = 2.36\lambda_0$  and  $t_{q=1} = 2.93\lambda_0$  for each design, respectively.

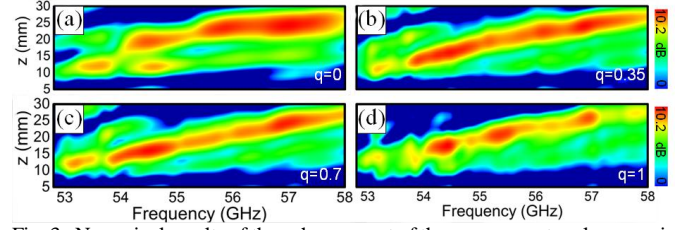


Fig. 3. Numerical results of the enhancement of the power spectra along  $z$ -axis (i.e., optical axis) for the designs: (a)  $q=0$ , (b)  $q=0.35$ , (c)  $q=0.7$  and (d)  $q=1$ .

and  $0.8\lambda_0$ , respectively.

The resulting zoned profile for each lens is calculated using (2), see Fig. 2. The design  $q = 0$  comprises 7 zones, whereas the rest have 6 zones. All the metalenses are designed with perforated metallic layers with  $37 \times 23$  holes and lateral dimensions of  $21\lambda_0 \times 21.7\lambda_0$  (111mm  $\times$  115mm) along  $x$  and  $y$  axes, respectively. The thickness of each metalens is shown in the caption of Fig. 2 where a total number of layers (the elementary three common layers at their center and those due to the zones) along  $z$ -axis of 6, 9, 9, and 11 is used for the  $q = 0, 0.35, 0.7$  and  $1$  designs, respectively.

### C. Simulation result: focusing performance

The focusing performance of the designs was studied numerically using the commercial software CST Microwave Studio<sup>TM</sup> with the procedure described in [7]. The metal used was aluminum with finite conductivity  $\sigma_{Al} = 3.56 \times 10^7$  S/m. Given the symmetry of the problem, electric and magnetic symmetries were used at  $xz(H)$ - and  $yz(E)$ - planes, respectively. A hexahedral mesh with a resolution up to  $0.056\lambda_0 \times 0.056\lambda_0 \times 0.028\lambda_0$  along  $x$ -,  $y$ - and  $z$ - axis, respectively, was used.

The numerical results of the power enhancement (defined as the power received with and without the metalens) spectra along the metalenses' optical axis are shown in Fig. 3. The maximum (all values normalized to the maximum case,  $q = 0.35$ , are listed in Table I) emerges for all cases slightly above ( $\sim 0.25$  GHz)  $f = 56.7$  GHz, which represents only a 0.44% deviation with the ray tracing design. This could be due to the discretization of the profiles along all directions due to the unit cell used [14] or to the simplification of the design by using the effective refractive index of an infinite stack, instead of that of a finite stack [9], [14]. The corresponding focal lengths are summarized in Table I. They all show good agreement with the theoretical value ( $FL = 4.5\lambda_0$ ).

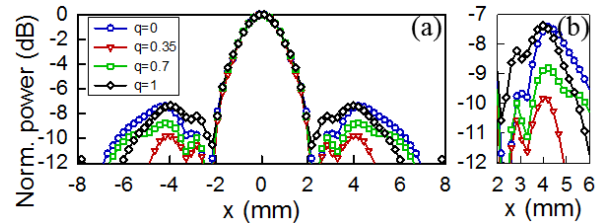


Fig. 4. (a) Numerical results of the normalized power distribution along the transversal  $x$ -axis at each numerical  $FL$  for the zoned fishnet metalenses with  $q = 0$  (circle),  $q = 0.35$  (triangles),  $q = 0.7$  (squares) and  $q = 1$  (diamonds). (b) Zoom-in of the SLL from (a).

TABLE I

SIMULATIONS RESULTS OF THE FOCUSING PERFORMANCE AT 56.7 GHz

Metals design	FL <sup>a</sup> ( $\lambda_0$ )	FL Error (%)	NP <sup>b</sup> at each FL (dB)	SLL <sup>c</sup> (dB)	First null (dB)
$q = 0$	4.57	1.56	-0.3	7.5	16.2
$q = 0.35$	4.52	0.44	0	9.7	17
$q = 0.7$	4.42	1.78	-0.07	8.6	14.3
$q = 1$	4.80	6.67	-0.72	7.5	10.6

<sup>a</sup>FL is the Focal length.<sup>b</sup>NP is the normalized power.<sup>c</sup>SLL is the side lobe level.

The normalized power distribution along the transversal  $x$ -axis at each  $FL$  for  $f = 56.7$  GHz is displayed in Fig. 4 (results normalized to the maximum of each case). The full-width at half maximum (FWHM) is preserved for all cases with a value of  $\sim 0.43\lambda_0$ . Furthermore, as Table I shows, the reference phase modulates the SLL as well as the first null. For our particular fishnet design,  $q = 0.35$  provides the best results among all.

### III. FABRICATION AND EXPERIMENTS

In light of the findings from the previous section, we opt to fabricate the most representative designs  $q = 0$  and  $0.35$ . The former case serves as a reference, whereas  $q = 0.35$  is meant to show the advantages of tuning the reference phase. The prototypes are made of aluminum using laser-cutting and the metal plates are stacked and separated by a 5 mm wide frame with screws, see Fig. 5 (a,b).

Measurements were performed using an AB Millimetre<sup>TM</sup> quasi-optical vector network analyzer (VNA) with the same setup described in [7], [9]: a high gain horn antenna was used as a transmitter and a standard flange-ended WR-15 waveguide was used as a receiver to raster scanning the  $xz$ -plane from the zoned face of the prototypes.

The power distribution along the optical  $z$ -axis was obtained by moving the receiver from 5 to 30 mm with a step of 0.25 mm. The  $FL$  for  $f = 56.7$  GHz were:  $FL_{exp,q=0} = 4.1\lambda_0$  and  $FL_{exp,q=0.35} = 4.2\lambda_0$  for  $q = 0$  and  $0.35$ , respectively. These values represent, respectively, a disagreement of 10.2% and 7.1% from the numerical ones, which may be due to fabrication tolerances.

The power distribution along the transversal  $x$ -axis was measured by moving the receiver along the  $x$ -axis from -10 mm to 10 mm with a step of 0.5 mm, see results in Fig. 5. A qualitative good agreement between simulation and experimental results is evident by comparing Figs. 4 and 5, with a reduction of SLL and a deep first null for  $q = 0.35$  compared to  $q = 0$ . Note that the foci in the experimental cases are not completely symmetric, which may be due to fabrication tolerances such as unavoidable bends of the metal plates; also, even though the experiment was set up with the best possible care, some misalignments between the receiver, lens and transmitter may be present. The experimental full-width at half-maximum are  $FWHM_{exp,q=0} = 0.42\lambda_0$  and  $FWHM_{exp,q=0.35} = 0.61\lambda_0$  for the designs  $q = 0$  and  $0.35$ , respectively. In simulation  $FWHM = 0.43\lambda_0$  was obtained for both designs. The experimental SLL is  $\sim 10$  dB and  $\sim 12.5$  dB below the main lobe for the designs  $q = 0$  and  $0.35$ ; i.e., a reduction of 2.5 dB in the

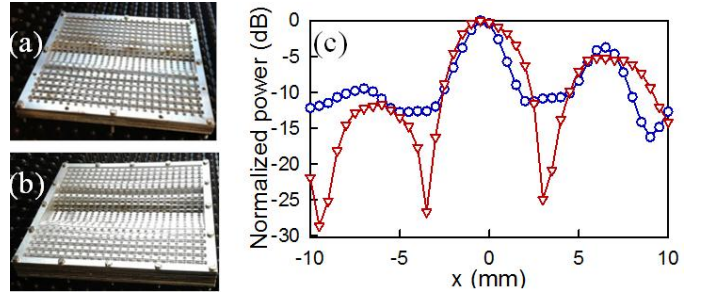


Fig. 5. Fabricated prototypes with  $q=0$  (a) and  $q=0.35$  (b). (c) Experimental results of the normalized power distribution along the transversal  $x$ -axis at each  $FL$  for the zoned fishnet metalenses with  $q = 0$  (circles) and  $q = 0.35$  (triangles).

SLL is obtained when the reference phase of  $0.7\pi$  is applied to the zoned fishnet metalenses, in good agreement with the theoretical predictions.

Because of reciprocity arguments, a zoned fishnet metalenses antenna configuration should also benefit from the reference phase tuning (as it was demonstrated in [12], [16] for circular planar Fresnel zone plate antennas). CST Microwave Studio<sup>TM</sup> is used again to investigate numerically such hypothesis. The realistic flange-ended WR-15 waveguide was used as a transmitter. It was fully modeled and placed at the  $FL$  obtained from simulation results for each design. Hence, the metalenses were illuminated from their profiled face. The same minimum mesh size as previously was used.

For the experimental characterization, the prototypes were placed between a standard flange-ended WR-15 waveguide and a high gain horn antenna. The former was used as a feeder and was located at each experimental  $FL$  ( $FL_{exp,q=0} = 4.1\lambda_0$  and  $FL_{exp,q=0.35} = 4.2\lambda_0$ ). The latter acted as a receiver and was placed 4000 mm apart from the flat face. Both, transmitter and metalens, were fixed on a rotatory platform in order to perform the angular scan from  $-90^\circ$  to  $+90^\circ$  with a step of  $0.5$  deg. Measurements were carried out using the AB Millimetre<sup>TM</sup>

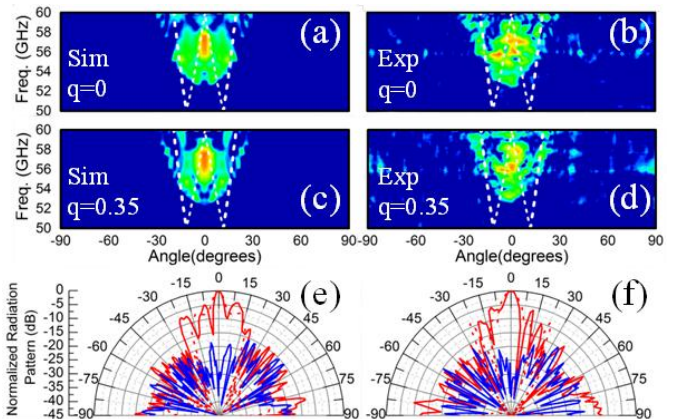


Fig. 6. Numerical (a, c) and experimental (b, d) co-polar radiation pattern as a function of frequency for the zoned fishnet metalens designed with factor:  $q = 0$  (a-b) and  $q = 0.35$  (c-d), respectively. The white dashed lines plotted in panels (a-d) are the analytic angular positions of the first order grating lobes (0,-1), (-1,0) and (-1,1) [8]. Results of the normalized radiation pattern at  $f = 56.7$  GHz for the simulated (red dashed line) and experimental (red solid line) results of the co-polarization along with the measured cross-polarization (blue solid line) of the designed zoned fishnet metalenses using reference phase with factor: (e)  $q = 0$  and (f)  $q = 0.35$ , respectively.

TABLE II  
SIMULATIONS AND EXPERIMENTAL RESULTS OF THE RADIATION  
PERFORMANCE AT 56.7 GHz

ML <sup>a</sup> (q)	$\theta_{-3dB}$ <sup>b</sup> Sim (deg)	$\theta_{-3dB}$ <sup>b</sup> Exp (deg)	SLL <sup>c</sup> Sim (dB)	SLL <sup>c</sup> Exp (dB)	G <sup>d</sup> Sim (dB)	G <sup>d</sup> Exp (dB)	BW <sup>e</sup> Sim (GHz)	BW <sup>e</sup> Exp (GHz)
0	4.8	4.5	7.35	3.91	13.23	9.53	2.3	1.96
0.35	6	5	11	6.31	13.71	11.3	2.5	1.2

<sup>a</sup>ML is the metalens design

<sup>b</sup> $\theta_{-3dB}$  is the -3dB beamwidth.

<sup>c</sup>SLL is the side lobe level

<sup>d</sup>G is the gain.

<sup>e</sup>BW is the -3dB bandwidth calculated from the gain values.

VNA. Notice that the WR-15 waveguide pattern has not been de-embedded from the experimental results which may strongly influence the performance of the lens antenna (and also in the focal plane measurements)

Simulation and experimental results of the radiation pattern of the co-polar component on the  $xz(H)$ -planes as a function of frequency and angle are shown in Fig. 6 (a-b) for  $q = 0$  and in Fig. 6(c-d) for  $q = 0.35$ . Again, good agreement between simulation and experimental results is obtained. It is important to remark that, given the -12 dB edge taper criterion followed in this manuscript, spillover side lobes do not appear here, at difference from [8]. From simulation results, a gain of 13.23 dB and 13.71 dB is obtained at  $f = 56.7$  GHz for the designs  $q = 0$  and 0.35, respectively. The experimental gain was obtained by applying the gain comparison method [17]. The resulting value is slightly lower than simulation results with values of 9.53 dB and 11.30 dB at the working frequency. However, note that in both, simulation and experimental results, the gain obtained for  $q = 0.35$  is always higher than that for  $q = 0$ .

To better compare the results obtained from simulation and measurements, the co- (y) and cross-polar (x) components of the normalized radiation pattern at the operational frequency for both designs,  $q = 0$  and 0.35, are shown in Fig. 6 (e) and (f), respectively, and a summary of the radiation pattern characteristics is shown in Table II. The resulting simulated and experimental main lobe half-power beamwidth ( $\theta_{-3dB}$ ) values are similar in both cases. Regarding the first SLL, the experimental values for both metalenses are higher than the values obtained from numerical simulations. However, a reduction of  $\sim 2.4$  dB of the first side lobe is achieved experimentally when a reference phase with factor  $q = 0.35$  is used (compared with the SLL when no reference phase is used,  $q = 0$ ). These results demonstrate that the reference phase concept applied along with the zoning technique improve also the level of the first side lobe in a lens-antenna configuration.

#### IV. CONCLUSION

In this paper, the concept of reference phase introduced for Fresnel zone plate antennas has been applied to a zoned fishnet metalens. The focusing properties of several designs with different reference phase factors  $q = 0, 0.35, 0.7$  and 1 (corresponding to a reference phase of 0,  $0.7\pi$ ,  $1.4\pi$  and  $2\pi$ , respectively) has been presented. Simulation results demonstrate that the higher power intensity at the focal length and lower first side lobe level are achieved for the design with

factor  $q = 0.35$ . Also,  $q = 0.35$  shows better radiation characteristics than the rest in a lens antenna configuration. Stimulated by these numerical studies,  $q = 0$  and 0.35 have been fabricated. The  $q = 0.35$  outperforms  $q = 0$  in focusing and radiation properties. The measurements to characterize the focal plane show a reduction of 2.5 dB in the first SLL, whereas an improvement of 2.4 dB and 1.77 dB in the first SLL and gain, respectively, is reported in the radiation pattern experiments. The results here proposed may be used in the design of advanced zoned lenses made of artificial materials aiming at improving the performance of lens antenna systems.

#### REFERENCES

- [1] N. Llombart and A. Neto, "THz Time-Domain Sensing: The Antenna Dispersion Problem and a Possible Solution," *IEEE Trans. Terahertz Sci. Technol.*, vol. 2, no. 4, pp. 416–423, 2012.
- [2] A. Demetriadou and Y. Hao, "A Grounded Slim Luneburg Lens Antenna Based on Transformation Electromagnetics," *IEEE Antennas Wirel. Propag. Lett.*, vol. 10, pp. 1590–1593, 2011.
- [3] G. Savini, P. A. R. Ade, and J. Zhang, "A new artificial material approach for flat THz frequency lenses," *Opt. Express*, vol. 20, no. 23, pp. 25766–25773, 2012.
- [4] J. Neu, R. Beigang, and M. Rahm, "Metamaterial-based gradient index beam steerers for terahertz radiation," *Appl. Phys. Lett.*, vol. 103, no. 4, pp. 041109–1–4, 2013.
- [5] M. Beruete, M. Sorolla, M. Navarro-cía, and F. Falcone, "Extraordinary transmission and left-handed propagation in miniaturized stacks of doubly periodic subwavelength hole arrays," *Opt. Express*, vol. 15, no. 3, pp. 1107–1114, 2007.
- [6] V. Torres, P. Rodríguez-Ulibarri, M. Navarro-Cía, and M. Beruete, "Fishnet metamaterial from an equivalent circuit perspective," *Appl. Phys. Lett.*, vol. 101, no. 24, p. 244101, 2012.
- [7] V. Pacheco-Peña, B. Orazbayev, V. Torres, M. Beruete, and M. Navarro-Cía, "Ultra-compact planoconcave zoned metallic lens based on the fishnet metamaterial," *Appl. Phys. Lett.*, vol. 103, no. 18, p. 183507, 2013.
- [8] V. Pacheco-Peña, B. Orazbayev, U. Beaskoetxea, M. Beruete, and M. Navarro-Cía, "Zoned near-zero refractive index fishnet lens antenna: Steering millimeter waves," *J. Appl. Phys.*, vol. 115, pp. 124902–1–8, 2014.
- [9] B. Orazbayev, V. Pacheco-Peña, M. Beruete, and M. Navarro-Cía, "Exploiting the dispersion of the double-negative-index fishnet metamaterial to create a broadband low-profile metallic lens," *Opt. Express*, vol. 23, no. 7, pp. 8555–8564, 2015.
- [10] H. D. Hristov, *Fresnel Zones in Wireless Links, Zone Plate Lenses and Antennas*. Inc., Norwood, MA: Artech House, 2000.
- [11] M. Born and E. Wolf, *Principles Of Optics*, 7th ed. New York: Cambridge University Press, 1999.
- [12] I. V. Minin and O. V. Minin, "Reference Phase in Diffractive Lens Antennas: A Review," *J. Infrared, Millimeter, Terahertz Waves*, vol. 32, no. 6, pp. 801–822, Apr. 2011.
- [13] M. Navarro-Cía, M. Beruete, I. Campillo, and M. Sorolla, "Beamforming by Left-Handed Extraordinary Transmission Metamaterial bi-and plano-concave lens at millimeter-waves," *IEEE Trans. Antennas Propag.*, vol. 59, no. 6, pp. 2141–2151, 2011.
- [14] M. Beruete, M. Navarro-Cía, M. Sorolla, and I. Campillo, "Planoconcave lens by negative refraction of stacked subwavelength hole arrays," *Opt. Express*, vol. 16, no. 13, pp. 9677–9683, 2008.
- [15] C. A. Balanis, *Antenna theory: analysis and design*, Third Edit., vol. 72. Hoboken, New Jersey: John Wiley & Sons, 2005.
- [16] S. M. Stout-Grandy, A. Petosa, I. V. Minin, O. V. Minin, and J. Wight, "A Systematic Study of Varying Reference Phase in the Design of Circular Fresnel Zone Plate Antennas," *IEEE Trans. Antennas Propag.*, vol. 54, no. 12, pp. 3629–3637, 2006.
- [17] "IEEE Standard Test Procedures for Antennas, 149-1979," *IEEE Stand. Test Proced. Antennas, ANSI/IEEE Stand. 149-1979*, 1979.